ACS APPLIED MATERIALS & INTERFACES

Research Article

www.acsami.org

Fluorogen–Peptide Conjugates with Tunable Aggregation-Induced Emission Characteristics for Bioprobe Design

Ruoyu Zhang,[†] Youyong Yuan,[†] Jing Liang,[†] Ryan T. K. Kwok,[‡] Qing Zhu,[§] Guangxue Feng,[†] Junlong Geng,[†] Ben Zhong Tang,[‡,∥] and Bin Liu*[,†,⊥]

[†]Department of Chemical and Biomolecular Engineering, National University of Singapore, 4 Engineering Drive 4, Singapore 117576

[‡]Department of Chemistry, Division of Biomedical Engineering, The Hong Kong University of Science and Technology, Clear Water Bay, Kowloon, Hong Kong, China

[§]Institute of Bioengineering, Zhejiang University of Technology, Chaowang Road 18, Hangzhou 310014, China

[∥]SCUT-HKUST Joint Research Laboratory, Guangdong Innovative Research Team, State Key Laboratory of Luminescent Materials and Devices, South China University of Technology, Guangzhou 510640, China

[⊥]Institute of Materials Research Engineering, 3 Research Link, Singapore 117602

Supporting Information

ABSTRACT: Fluorogens with aggregation-induced emission (AIE) characteristics are attracting intense research interest, and an AIE–peptide conjugate strategy has been reported for developing turn-on probes based on hydrophilic peptide ligands. To build a model also suitable for hydrophobic ligands, we propose to fine-tune the AIE characteristics for probe design. In this work, an iconic AIE fluorogen tetraphenylethene (TPE) was designed to conjugate with peptide fragments containing different numbers of aspartic acid (D) units. Relationships between the numbers of D and the hydrophilicity, optical properties, and aggregate sizes and the AIE characteristics of TPE–peptide conjugates were investigated carefully. Five carboxyl groups were found to be the threshold to "turn off" the fluorescence of TPE. As a proof-of-concept, TPE-SS-D_5 containing a cleavable disulfide bond was synthesized for thiol turn-on detection. The validated tunable AIE characteristic offers new opportunities to design fluorescence turn-on probes based on hydrophobic recognition elements and AIE fluorogens.

KEYWORDS: *light-up probe, aggregation-induced emission, fluorescent probes, thiol detection, tetraphenylethene*

INTRODUCTION

Fluorescence technique has become one of the most powerful tools for biosensing and bioimaging due to its advantages such as high sensitivity, easy operation, and versatile functions.[1−4] Several design strategies including photoinduced electron transfer (PET),[5−7] internal charge transfer (ICT),[8,9] and fluorescence resonance energy transfer (FRET)[10−13] have been well established and applied to the development of various fluorescence turn-on probes. These probes are highly desirable for biosensor applications due to their higher sensitivity and more accurate results than those of fluorescence turn-off probes, especially for trace detection of analytes in complicated systems.[14−16]

Recently, fluorogens with aggregation-induced emission (AIE) characteristics have attracted intense research interest as a novel class of optical materials.[17−20] AIE fluorogens are rotor-type molecules that show weak fluorescence in solution state but emit strong fluorescence in aggregate state.[21,22] Mechanistic studies suggest that, in solution, the free motion of the rotor structures (e.g., phenylene rings) consumes the excited state energy by nonradiative decay to quench the emission.[23] When the molecules are aggregated, the block of the intramolecular motion will activate the radiative decay pathway to yield strong fluorescence. Unlike traditional organic fluorogens suffering from aggregation-caused quenching, the nature of AIE fluorogens permits the use of highly concentrated solution and offers higher sensitivity and better photobleaching-resistance for biological applications.[24]

There have been a number of chemo/biosensors reported based on AIE fluorogens[25] for the detection of proteins,[26−33] DNA,[34] heparin,[35,36] and biological thiols.[37−40] A majority of the current turn-on probes are based on cationic/anionic AIE fluorogens, and their fluorescence turn-ons are due to electrostatic or hydrophobic interactions with analytes. This mechanism limits their detection selectivity, and most of these assays only response to individual purified analyte in solution, as other charged molecules could easily bring interference. Recently, to develop highly specific AIE-fluorogen-based bioprobes, we reported an AIE–peptide conjugate strategy by the incorporation of specific peptide-based recognition

Received: June 7, 2014
Accepted: July 29, 2014
Published: July 29, 2014

elements to AIE fluorogens for integrin and caspase activity studies.[41−45] The same strategy has also been proved effective for cancer cell detection.[46] These probes are highly specific and sensitive because (1) the introduction of hydrophilic ligand makes the bioprobes soluble in aqueous media as molecular species, which are nonemissive with extremely low background signals, and (2) upon specific binding to analyte or in the presence of a biological event, the fluorescence of AIE fluorogens is recovered, offering both high selectivity and high signal output. As the background signal is highly dependent on the water-solubility of the probe, the design strategy is limited to the selection of highly hydrophilic recognition element for each probe. It is thus of high importance to understand the effect of peptide moiety on fine-tuning the aggregation-induced emission characteristics of AIE fluorogens.

To build a model for such a study, we propose to synthesize a series of AIE fluorogen−peptide conjugates with different numbers of amino acids in each sequence. In this contribution, AIE−peptide conjugates TPE-D_n (n = 1−5) were synthesized using an iconic AIE fluorogen tetraphenylethene (TPE) and peptide fragments consisting of different numbers of aspartic acid (D). Relationships between the numbers of D units and the hydrophilicity, optical properties, and aggregate sizes and the AIE characteristics of TPE−peptide conjugates were investigated carefully to find the threshold number of D units needed to achieve the "off" state. As a proof-of-concept, TPE-SS-D_5 was designed for light-up thiol detection by inserting a linker containing a cleavable disulfide bond between TPE and D_5. This study offers new opportunities to design AIE-fluorogen-based fluorescence turn-on probes containing hydrophobic recognition elements.

EXPERIMENTAL SECTION

Chemicals and Instruments. Anhydrous dimethyl sulfoxide (DMSO), dimethylformamide (DMF), dichloromethane (DCM), acetonitrile (CH_3CN), dithiobis(succinimidyl propionate) (DSP), *N,N*-diisopropylethylamine (DIEA), triethylamine (TEA), glutathione (GSH), triisopropylsilane (TIS), trifluoroacetic acid (TFA), piperidine, 1-octanol, and 1-hydroxybenzotriazole hydrate (HOBt) were purchased from Sigma-Aldrich. *N,N,N′,N′*-tetramethyl-*O*-(1*H*-benzotriazol-1-yl)uronium hexafluorophosphate (HBTU) was purchased from Biochem. Boc-L-aspartic acid(4-*tert*-butyl)ester was purchased from Fluka. All chemicals and reagents were used without further purification. Deuterated dimethyl sulfoxide (DMSO-d_6) was purchased from Cambridge Isotope Laboratories, and peptides with sequences of Asp-Asp (D_2), Asp-Asp-Asp (D_3), Asp-Asp-Asp-Asp (D_4), and Asp-Asp-Asp-Asp-Asp (D_5) were customized from GL Biochem Ltd. Milli-Q water was supplied by a Milli-Q Plus System (Millipore Corp., Billerica, MA).

UV−vis absorption spectra were recorded on a Shimadzu UV-1700 spectrometer. Photoluminescence (PL) spectra were measured on a PerkinElmer LS 55 spectrofluorometer equipped with a xenon lamp excitation source and a Hamamatsu (Japan) 928 PMT, using 90° angle detection for solution samples. The size and size distribution of particles were determined by laser light scattering (LLS) with a particle size analyzer (90 Plus, Brookhaven Instruments Co., Holtsville, NY) at a fixed angle of 90° at room temperature. Atomic force microscopy (AFM) was performed on a Digital Instrument Nanoscope IIIa scanning probe microscope operated in the tapping mode. Nuclear magnetic resonance (NMR) spectra were acquired on a Bruker ARX 400 NMR spectrometer or Varian 600 MHz NMR spectrometer. High-performance liquid chromatography (HPLC) profiles were acquired using an Agilent 1100 Series HPLC System. The mass spectra were measured using a Shimadzu IT−TOF system.

Synthesis of 1-[4-(Isothiocyanatomethyl)phenyl]-1,2,2-triphenylethene (TPE-NCS). TPE-NCS was synthesized according to the literature with 85% yield.[47] ^{1}H NMR ($CDCl_3$, 400 MHz): 7.13−6.89 (m, 19H), 4.63 (s, 2H). HRMS (MALDI-TOF) m/z: 403.1386 ($[M]^+$ calcd, 403.1395).

Synthesis of TPE-D_n (n = 1−5). First, D-NH_2 was synthesized using Fmoc strategy with rink amide resin as the solid support, as shown in Scheme S2 (Supporting Information). The resin (150 mg, loading ∼0.5 mmol/g) was first swelled in DMF for 1 h and then deprotected in piperidine/DMF (v/v = 1/4) for 2 h at room temperature. The piperidine was removed, and the resin was washed with DMF and DCM and dried thoroughly by high vacuum. Next, the dry resin was added into the mixture of Boc-L-aspartic acid(4-*tert*-butyl)ester (92 mg) together with HOBt (4 equiv), HBTU (4 equiv), and DIEA (8 equiv) dissolved in 1.5 mL dry DMF. The resulting mixture was shaken at room temperature for 12 h. Then, the resin was filtered and washed with DMF (10 mL, three times), DCM (10 mL, three times), and DMF (10 mL, three times) until the filtrate became colorless. After drying under vacuum, the resin was deprotected again with 5 mL of piperidine/DMF (v/v = 1:4). The peptide was finally cleaved in 3 mL of TFA/TIS/H_2O (v/v/v = 95:2.5:2.5) for 3 h at room temperature to yield the product of D-NH_2 in 70% yield. ESI-MS, m/z: 131.0398 ($[M - H]^-$ calcd, 131.0457).

TPE-D was synthesized in a typical reaction. Into a mixture of TPE-NCS (6.61 mg, 16.4 μmol) and D-NH_2 (3.25 mg, 24.6 μmol) in 0.5 mL of DMSO, was added 3 μL of DIEA, and the mixture was stirred at room temperature for 24 h. The final product was purified by prep-HPLC and lyophilized under vacuum to give the product as a white powder in 40% yield (3.51 mg). ^{1}H NMR (DMSO-d_6, 600 MHz): 7.84 (t, J = 6.0 Hz, 1H), 7.13−6.87 (m, 18H), 4.68 (d, J = 6.0 Hz, 2H), 2.48−2.47 (d, 2H, overlap with DMSO-d_6). ESI-MS, m/z: 1093.3503, ($[2\ M + Na]^+$ calcd, 1093.3757). TPE-D_2 was synthesized from TPE-NCS (7.26 mg, 16.4 μmol) and D_2-COOH (6.67 mg, 24.6 μmol) dissolved in DMSO (0.5 mL) with a catalytic amount of DIEA (3 μL). The mixture was stirred at room temperature for 24 h and purified in the same way to give the product as a white powder in 38% yield (4.06 mg). ^{1}H NMR (DMSO-d_6, 600 MHz): 8.20 (m, 2H), 7.69 (d, J = 12.0 Hz, 1H), 7.15−6.90 (m, 19H), 5.15 (s, 2H), 4.57−4.47 (m, 2H), 2.65−2.55 (m, 4H, overlap with DMSO-d_6). ESI-MS, m/z: 652.1965 ($[M + H]^+$ calcd, 652.2117). TPE-D_3 was synthesized from TPE-NCS (5.42 mg, 13.43 μmol) and D_3-COOH (7.31 mg, 20.14 μmol) in 39% yield (4.02 mg). ^{1}H NMR (DMSO-d_6, 600 MHz): 8.29 (d, J = 6.0 Hz, 1H), 8.18−8.04 (m, 1H), 7.88 (d, J = 6.0 Hz, 1H), 7.70 (d, J = 6.0 Hz, 1H), 7.21−6.90 (m, 19H), 5.03 (s, 1H), 4.61−4.48 (m, 3H), 2.73−2.48 (m, 6H, overlap with DMSO-d_6). ESI-MS, m/z: 767.2217, ($[M + H]^+$ calcd, 767.2387). TPE-D_4 was synthesized from TPE-NCS (4.42 mg, 10.95 μmol) and D_4-COOH (7.85 mg, 16.43 μmol) in 42% yield (4.05 mg). ^{1}H NMR (DMSO-d_6, 600 MHz): 8.29 (d, J = 6.0 Hz, 1H), 8.09 (m, 1H), 7.93 (d, J = 6.0 Hz, 1H), 7.86 (d, J = 6.0 Hz, 1H), 7.67 (d, J = 6.0 Hz, 1H), 7.15−6.90 (m, 19 H), 5.04 (s, 1H), 4.57−4.48 (m, 4H), 2.72−2.48 (m, 8H, overlap with DMSO-d_6). ESI-MS, m/z: 920.1834 ($[M + K]^+$ calcd, 920.2215). TPE-D_5 was synthesized from TPE-NCS (5.48 mg, 13.57 μmol) and D_5-COOH (12.06 mg, 16.43 μmol) in 40% yield (5.42 mg). ^{1}H NMR (DMSO-d_6, 600 MHz): 8.31 (d, J = 6.0 Hz, 1H), 8.11 (m, 1H), 7.98−7.90 (m, 3H), 7.69 (d, J = 6.0 Hz, 1H), 7.16−6.90 (m, 19 H), 5.05 (s, 1H), 4.54−4.45 (m, 5H), 2.73−2.48 (m, 10H, overlap with DMSO-d_6). ESI-MS, m/z: 1019.2378 ($[M + Na]^+$ calcd, 1019.2745).

Synthesis of 1-[(4-Aminomethyl)phenyl]-1,2,2-triphenylethene (TPE-NH_2). A solution of 1-[(4-azidomethyl)phenyl]-1,2,2-triphenylethene (TPE-N_3) (0.116 g, 0.3 mmol) and triphenylphosphine (0.118 g, 0.45 mmol) in 6 mL anhydrous methanol was added into a 50 mL two-necked round bottle flask under nitrogen protection.[48] The mixture was refluxed for 12 h and then cooled to room temperature followed by evaporation under reduced pressure. The crude product was purified by silica-gel chromatography to yield TPE-NH_2 as a white powder in 70% yield (0.13 g). ^{1}H NMR ($CDCl_3$, 400 MHz): 7.13−6.87 (m, 19H), 3.82 (s, 2H), 1.23 (m, 2H). HRMS (MALDI-TOF) m/z: 361.1833 ($[M]^+$ calcd, 361.1830).

Scheme 1. Synthetic Route to AIE–Peptide Conjugates TPE-D$_n$ (n = 1–5)

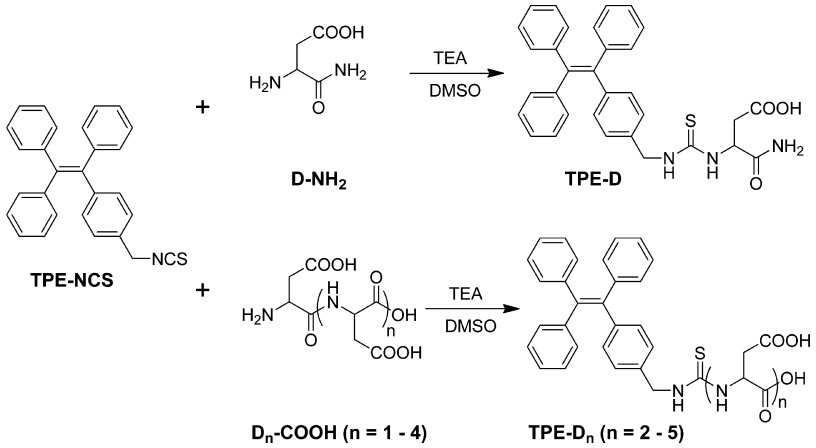

Synthesis of TPE-SS-D$_5$. TPE-SS-D$_5$ was synthesized according to the literature.[48] Into a mixture of TPE-NH$_2$ (5.90 mg, 15.22 μmol) and D$_5$-COOH (8.98 mg, 15.22 μmol) in DMSO (0.5 mL), was added 2 μL of DIEA, and the mixture was stirred for 10 min at room temperature. Then, DSP (6.13 mg, 15.22 μmol) in 0.5 mL of DMSO was quickly added, and the mixture was stirred for another 24 h at room temperature. The final product was purified by prep-HPLC and lyophilized under vacuum to give the product as a white powder in 49% yield (8.43 mg). ^{1}H NMR (DMSO-d_6, 600 MHz): 8.34–7.87 (m, 6H), 7.14–6.87 (m, 19H), 4.53–4.44 (m, 5H), 4.17–4.16 (d, 2H), 2.88–2.81 (m, 4H), 2.69–2.41 (m, 14H, overlap with DMSO-d_6). ESI-MS, m/z: 1127.3131 ([M − H]$^-$ calcd, 1127.3014).

Synthesis of TPE-SS-COOH. TPE-SS-COOH was synthesized in a similar way as TPE-SS-D$_5$ but without the addition of D$_5$. The final product was also purified by prep-HPLC (solvent A, water with 0.1% TFA; solvent B, CH$_3$CN with 0.1% TFA) and lyophilized under vacuum to give the product as a white powder in 30% yield (4.35 mg). ^{1}H NMR (DMSO-d_6, 400 MHz): 8.38 (t, 1H), 6.89–7.15 (m, 19 H), 4.19 (d, 2H), 2.79–3.07 (m, 8H). ESI-MS, m/z: 552.1724 ([M − H]$^-$ calcd, 552.1667).

Titration of TPE-NCS and TPE-D$_n$ (n = 1–5). Mixtures (995 μL) of DMSO/H$_2$O with different water fractions were prepared. TPE-NCS and TPE-D$_n$ (n = 1–5) stock solutions were then added into the mixtures to give a final concentration of 10 μM. The PL spectra were obtained using a PerkinElmer LS 55 spectrofluorometer.

Measurement of Partition Coefficient. TPE-D$_n$ (n = 1–5) was dissolved in 1 mL of DMSO/H$_2$O (v/v = 1/199) mixtures (pH = 7.0, 1× PBS buffer) at a concentration of 10 μM and then partitioned with 1 mL of 1-octanol completely (for 24 h). The concentration of the TPE-D$_n$ in each phase was determined by absorption spectrum using Shimadzu UV-1700 spectrometer.

Laser Light Scattering Measurement. First, 6 μL of 10 mM TPE-NCS stock solution in DMSO was mixed with 9 μL of DMSO, which was then diluted with 2.985 mL of H$_2$O to yield a final concentration of 20 μM in 3 mL of DMSO/H$_2$O (v/v = 1/199). The stock solutions of TPE-D$_n$ (n = 1–5) were prepared in a similar method. The mixture was mixed thoroughly using a vortex mixer before LLS measurement using particle size analyzer.

Atomic Force Microscopy Measurement. First, 10 μM TPE-NCS and TPE-D$_n$ (n = 1–5) in DMSO/H$_2$O (v/v = 1/199) were mixed thoroughly using a vortex mixer before spin-coating onto a freshly cleaved mica surface. Then, the samples were dried in drying oven at 65 °C for 1 h and kept in vacuum oven for 1 h before they were imaged by tapping mode AFM.

General Procedure for Probe Activation by GSH. TPE-SS-D$_5$ (10 μM) was incubated with 1 mM GSH in 1 mL of DMSO/H$_2$O (v/v = 1/199) at room temperature, and the fluorescence spectra were measured at different time points (0, 10, 20, 30, 45, 60, 90, 180, and 360 min) to obtain time-dependent PL spectra. Next, GSH at different concentrations ranging from 1.0 μM to 1.0 mM were incubated with TPE-SS-D$_5$ for 3 h before fluorescence intensities were measured. The solutions were excited at 304 nm, and the emissions were collected from 390 to 575 nm.

RESULTS AND DISCUSSION

Synthesis of TPE-NCS and TPE–Peptide Conjugates (TPE-D$_n$, n = 1–5). The starting material, 1-[4-(isothiocyanatomethyl)phenyl]-1,2,2-triphenylethene (TPE-NCS; Scheme S1, Supporting Information), was synthesized as reported from 1-[(4-azidomethyl)phenyl]-1,2,2-triphenylethene (TPE-N$_3$) in 85% yield in the presence of triphenylphosphine (PPh$_3$) and CS$_2$ at 40 °C overnight.[47] The HRMS and the ^{1}H NMR, ^{13}C NMR spectra (Figures S1 and S2, Supporting Information) confirmed the right molecular structure of TPE-NCS. The synthesis of 2-diamino-4-oxobutanoic acid (amide terminated aspartic acid, D-NH$_2$) involves solid-phase chemistry as described in the Experimental Section and in Scheme S2 (Supporting Information). Briefly, deprotection of the Fmoc group on rink amide resin with 20% piperidine in dimethylformamide (DMF) (v/v = 1/4) for 2 h at room temperature yielded resin with active amine, which was coupled to Boc-L-aspartic acid(4-*tert*-butyl)ester to afford the aspartic-bearing resin. After deprotection of the amine groups, the product of D-NH$_2$ for further synthesis was obtained by cleavage from resin.

As shown in Scheme 1, TPE-D$_n$ (n = 1–5) was synthesized between TPE-NCS and amine functionalized D, D$_2$, D$_3$, D$_4$, and D$_5$ in the presence of a catalytic amount of triethylamine (TEA) in DMSO at room temperature for 24 h. After purification by HPLC and lyophilization, the products were characterized by ^{1}H NMR and ESI-MS (Figures S3–S7, Supporting Information). It is important to note that the terminal group of TPE-D is amide, while of the rest are carboxyl for TPE-D$_n$ (n = 2–5). As such, TPE-D$_n$ (n = 1–5) were endowed with one, three, four, five, and six carboxyl groups, respectively, for n = 1, 2, 3, 4, 5.

Optical Properties. The UV–vis absorption and PL spectra of TPE-D$_n$ were measured in the mixture of DMSO and H$_2$O (v/v = 1/199) at a concentration of 10 μM. The maximum absorption of TPE-NCS is at 314 nm, while all the TPE–peptide conjugates TPE-D$_n$ (n = 1–5) have the same absorption maxima at 304 nm, which is 10 nm blue-shifted in comparison with that of TPE-NCS. As seen from their PL spectra, TPE-NCS shows intense fluorescence at 480 nm (Figure 1A). This is due to aggregate formation in aqueous

dx.doi.org/10.1021/am5036048 | ACS Appl. Mater. Interfaces 2014, 6, 14302–14310

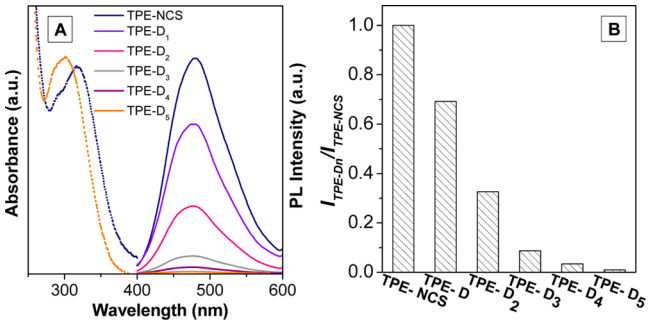

Figure 1. (A, dotted line) UV−vis absorption and (solid line) PL spectra of TPE-NCS and TPE-D$_n$ (n = 1−5). (B) Ratios of PL intensities of TPE-D$_n$ to TPE-NCS (measured in DMSO/H_2O (v/v = 1/199)). λ_{ex} (TPE-NCS) = 314 nm; λ_{ex} (TPE-D$_n$) = 304 nm; [TPE-NCS] = [TPE-D$_n$] = 10 μM.

media, which will be discussed later. Under the same conditions, TPE-D$_n$ (n = 1−5) shows similar emission maxima. However, there is an obvious decrease in the PL intensity with the increasing number of D units attached to the TPE. Specifically, for 10 μM TPE-D$_n$ (n = 1−5), if one uses $I_{TPE\text{-}Dn}/I_{TPE\text{-}NCS}$, where $I_{TPE\text{-}Dn}$ is the fluorescence intensity of TPE-D$_n$ and $I_{TPE\text{-}NCS}$ is the fluorescence intensity of TPE-NCS, to describe the fluorescence change, the ratios are 0.70, 0.35, and 0.08 for TPE-D$_1$, TPE-D$_2$, and TPE-D$_3$, respectively (Figure 1B). The ratios further reduce to 0.03 and 0.01, respectively, for TPE-D$_4$ and TPE-D$_5$, which emit very weak fluorescence in the same solvent mixture. We hypothesize that the low emission is due to the well-dissolved carboxyl groups that drive the intramolecular rotation of phenyl rings. To validate this hypothesis, we performed a series of tests to examine the dispersion status of TPE-D$_n$ in the mixture of DMSO and H_2O (v/v = 1/199).

AIE Properties of TPE-D$_n$. The AIE properties of TPE-NCS and TPE-D$_n$ (n = 1−5) were studied in DMSO/H_2O mixtures with different water fractions (f_w) to fine-tune the solvent polarity and the extent of aggregation. Each PL intensity measured was divided by its maximum PL intensity (i.e., the PL intensity when f_w = 99.5%) to get I/I_0 ranging from 0 to 1 (Figure 2). Generally, the AIE fluorogens are weakly emissive in good solvents such as DMSO, while the augment of water fraction induces a dramatic fluorescence increase. Accordingly, I/I_0 will experience an upward trend as the water fraction increases. As shown in Figure 2A and Figure S8A (Supporting Information), when the water fraction (f_w) varies from 0 to 40 vol %, the PL intensity of TPE-NCS remains at a very low level. As f_w changes from 40 to 60%, the PL intensity increases dramatically and I/I_0 goes from less than 0 to 0.8. Afterward, the PL intensity of TPE-NCS continues to increase gradually and reaches the maximum at 99.5 vol % water fraction. For TPE-D, its PL intensity remains very weak until f_w reaches 60 vol %. When f_w increases 60−80 vol %, the fluorescence intensity of TPE-D experiences a dramatic increase (I/I_0 increases from 0.05 to 0.9), which is followed by a slow saturation (Figure 2B and Figure S8B, Supporting Information). TPE-D$_2$ and TPE-D$_3$ also retain the typical AIE characteristics (Figure 2C,D and Figure S8C,D, Supporting Information); their PL intensities increase dramatically after the water fractions reach 70 and 80 vol %, respectively, and continue to increase until f_w is 99.5%. For TPE-D$_4$ and TPE-D$_5$, the PL intensities show some increase when f_w is larger than 80 and 90%, respectively, as shown in Figure 2E,F. It is noteworthy that although there is 5−10 fold fluorescence increase for TPE-

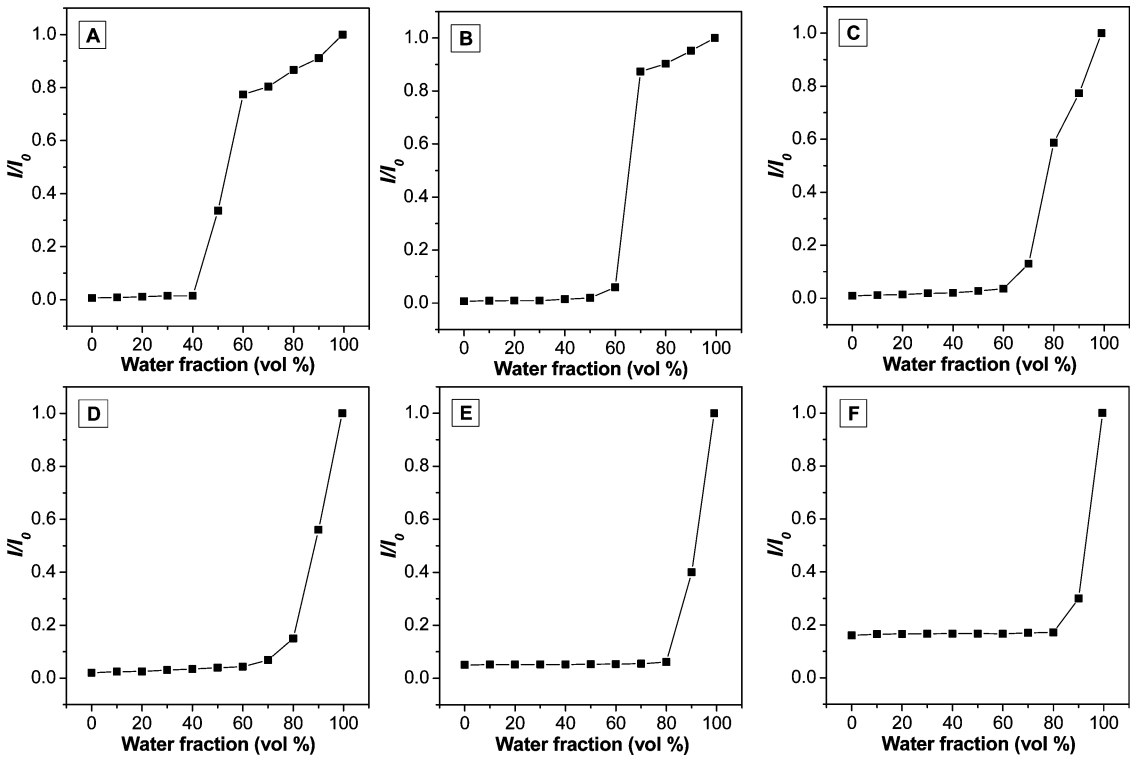

Figure 2. Plots of relative PL intensity (I/I_0) for (A) TPE-NCS, (B) TPE-D, (C) TPE-D$_2$, (D) TPE-D$_3$, (E) TPE-D$_4$, and (F) TPE-D$_5$ versus water fractions (f_w) in the DMSO/H_2O mixtures. I is PL intensity at any f_w, and I_0 is the PL intensity measured at f_w = 99.5%. λ_{ex} = 314 nm for TPE-NCS; λ_{ex} = 304 nm for TPE-D$_n$; [TPE-NCS] = [TPE-D$_n$] = 10 μM.

dx.doi.org/10.1021/am5036048 | ACS Appl. Mater. Interfaces 2014, 6, 14302−14310

D_4 and TPE-D_5 at f_w = 99.5% relative to f_w = 0%, their absolute fluorescence intensities remain low (Figure S8, panels E and F vs panels A and B, Supporting Information). The results show that the transition points of TPE-D_n at which molecules turn on their fluorescence are shifting to higher f_w values with the increasing number of D units in the conjugates. This further indicates that with an increasing number of D units, the TPE–peptide conjugates tend to show better dispersity in aqueous media.

It is well-known that the AIE properties are closely related to the state of fluorogens in solvents, in other words, the extent of aggregation. To explore the sizes of TPE-NCS and TPE-D_n (n = 1–5) aggregates in DMSO/H_2O (v/v = 1/199, 20 μM each), LLS and AFM were employed. As shown in Figure 3A, the

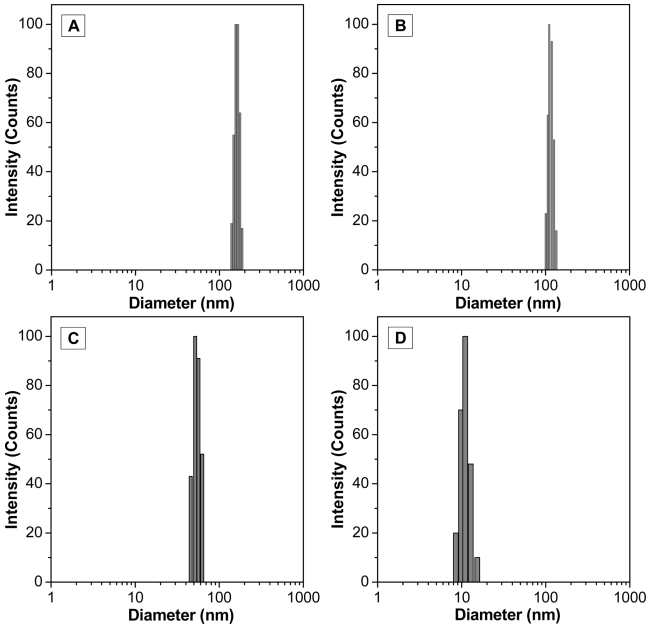

Figure 3. Hydrodynamic diameters of (A) TPE-NCS, (B) TPE-D, (C) TPE-D_2, and (D) TPE-D_3 (20 μM) in DMSO/H_2O (v/v = 1/199) measured by LLS.

hydrodynamic diameter of TPE-NCS aggregates is 160 ± 10 nm. In comparison, the hydrodynamic diameter of TPE-D aggregates decreases to 113 ± 8 nm (Figure 3B). By employing three and four carboxyl groups, the diameters of aggregates of TPE-D_2 and TPE-D_3 further decrease to 50 ± 4 and 12 ± 2 nm, respectively (Figure 3C,D). However, the sizes of TPE-D_4 and TPE-D_5 aggregates are too small to be detected precisely by LLS, indicating the good dispersity of the conjugates. These results revealed that peptide moieties could fine-tune the size of aggregates by improving the dispersity and solubility of TPE-D_n in aqueous media.

The morphologies and sizes of the aggregates were further studied by AFM. Suspensions of TPE-NCS and TPE-D_n (n = 1–5) conjugates were first prepared in the mixture of DMSO/H_2O (v/v = 1/199) at a concentration of 10 μM. Then, each suspension was spin-coated onto a freshly cleaved mica surface. All the AFM images were obtained under tapping mode. As shown in Figure 4, the aggregates show high uniformity in size at low magnification. In accordance with LLS results, the heights of TPE-D_n decrease as the number of D units increases, as evidenced in the height mode (Figure 4B,E,H,K,N,Q) and 3D mode (Figure 4C,F,I,L,O,R). Specifically, TPE-NCS aggregates are spherical in shape with a height of 30 nm (Figure 4A–C). The height of aggregates of TPE-D decreases to 20 nm. By employing three and four carboxyl groups, the heights of TPE-D_2 and TPE-D_3 decrease to 6 and 4 nm, respectively, indicating an improvement in dispersion. With five and six carboxyl groups, the height of TPE-D_4 aggregates further decreases to about 1 nm, and that for TPE-D_5 is even less than 1 nm. These results imply that with the aid of carboxyl groups, the aggregates of TPE-D_n become increasingly well-dispersed, which is most likely attributed to the improvement in hydrophilicity upon introduction of hydrophilic peptide moieties. Combined with PL spectra shown in Figure 1, the well-dispersed small dots of TPE-D_4 and TPE-D_5 on the mica surface demonstrate that five carboxyl groups are sufficient to impart good water-solubility to TPE molecules, as the dimensions of the dots are approaching the size of their single molecules.

Measurement of Partition Coefficients. The partition coefficient is defined as the ratio of concentrations of a compound in a mixture of two immiscible phases at equilibrium.[49−51] As shown in eq 1,

$$\text{partition coefficient} = \log \frac{[\text{solute}]_{\text{octanol}}}{[\text{solute}]_{\text{water}}} \quad (1)$$

the lipophilicity is reflected by a partition coefficient equal to the logarithm of the ratio of concentrations in octanol and water, log P. Positive values of log P indicate hydrophobicity of the compound while negative values indicate hydrophilicity. The greater the absolute value, the more hydrophobic or hydrophilic the compound is. In this work, partition coefficients were measured to explore the relationships between the numbers of carboxyl groups and the hydrophilicity of AIE–peptide conjugates. Generally, the log P values of TPE-NCS and TPE-D_n follow a linear declining trend in accordance with the number of carboxyl groups (Figure 5). The log P value of TPE-NCS was measured to be 0.86, indicating its high hydrophobicity. Hydrophobic TPE-NCS molecules form aggregates in water, and thus they are highly emissive in aqueous media. TPE-D has a log P value of ∼0.60, indicating that one carboxyl group is able to slightly reduce the hydrophobicity of a TPE molecule. With three carboxyl groups, the log P of TPE-D_2 was measured to be −0.27, revealing that the molecule is amphiphilic and hydrophilicity is slightly dominant. Accordingly, in Figure 1B, TPE-D_2 still shows 70% of florescence intensity of TPE-NCS under the same condition. The log P values for TPE-D_3 and TPE-D_4 were measured to be −0.63 and −0.81, respectively. The increased hydrophilicity of both correlated well with their low fluorescence in aqueous media. Finally, the log P value of TPE-D_5 reaches −1.08, which is clearly a hydrophilic molecule. This agrees with the previous observation that the fluorescence intensity of TPE-D_5 is the lowest in water. The linear trend shown in Figure 5 clearly demonstrates the successful strategy to fine-tune the solubility of TPE fluorogen by peptide conjugation.

Proof-of-Concept Bioprobe Based on TPE-SS-D_5 for Thiol Detection. The sensing of biological thiols is of great importance due to their vital role in many biological processes, and there have been several probes based on AIE fluorogens for thiol detection.[35−38] However, these probes require a high fraction (generally more than 50%) of organic solvents to eliminate background signal. It is highly desirable to develop AIE probes that are water-soluble. As discussed above, five

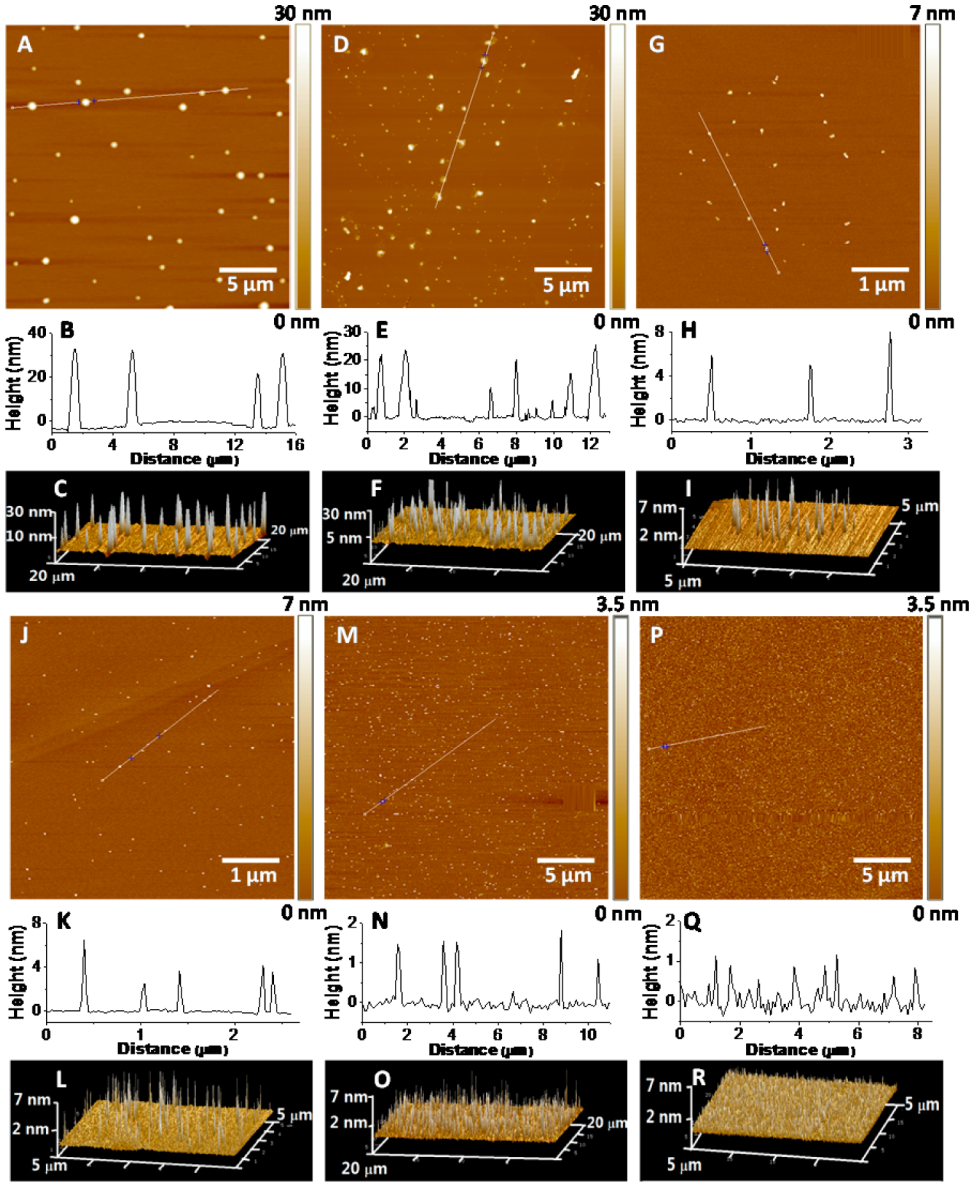

Figure 4. AFM images of (A–C) TPE-NCS, (D–F) TPE-D, (G–I) TPE-D_2, (J–L) TPE-D_3, (M–O) TPE-D_4, and (P–Q) TPE-D_5 after spin-coating their suspensions on a mica surface measured by tapping mode. (B, E, H, K, N, and Q) Height mode and (C, F, I, L, O, and R) corresponding 3D mode.

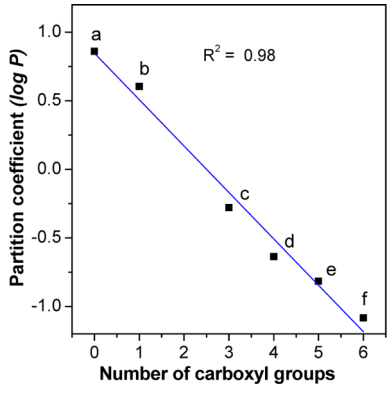

Figure 5. Partition coefficients of (a) TPE-NCS and (b–f) TPE-D_n (n = 1–5) as a function of the numbers of carboxyl groups they possess. TPE-NCS, TPE-D, TPE-D_2, TPE-D_3, TPE-D_4, and TPE-D_5 have zero, one, three, four, five, and six carboxyl groups, respectively.

carboxyl groups are a threshold to provide sufficient hydrophilicity to disperse the aggregates of TPE in aqueous media. Considering that TPE-D_5 shows the lowest fluorescence in aqueous media, it was selected for use in the development of a thiol probe as a proof-of-concept. A cleavable thiol responsive linker was inserted between TPE and the peptide moiety so that in the presence of thiols, the hydrophilic peptide moiety can be removed from TPE to recover the fluorescence.

As shown in Scheme 2, two probes, TPE-SS-D_5 and TPE-SS-COOH, were developed for thiol detection. The starting material of TPE-NH_2 (1-[(4-aminomethyl)phenyl]-1,2,2-triphenylethene) was synthesized in 70% yield by reducing TPE-N_3 using triphenylphosphine (PPh_3) under nitrogen protection.[48] Subsequently, TPE-SS-D_5 was synthesized through conjugation of TPE-NH_2 and D_5 in 49% yield using DSP as the linker. As the disulfide linker is thiol-specific and cleavable, in the presence of thiol species such as dithiothreitol (DTT) or glutathione (GSH), TPE-SS-D_5 is cleaved to induce the

dx.doi.org/10.1021/am5036048 | ACS Appl. Mater. Interfaces 2014, 6, 14302–14310

Scheme 2. Synthetic Route to TPE-SS-D_5 and TPE-SS-COOH

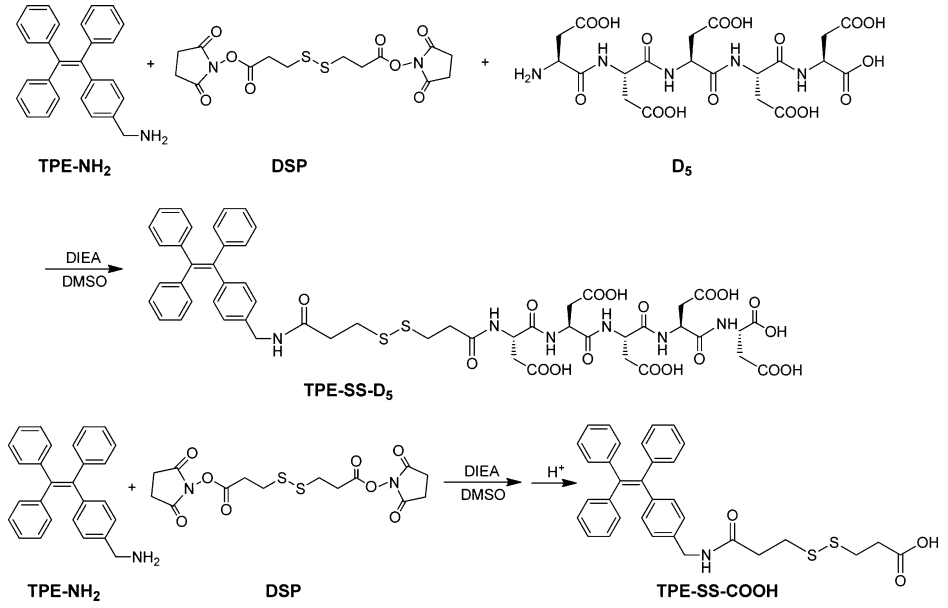

changes in water solubility, leading to evident fluorescence turn-on. Another probe, TPE-SS-COOH without the hydrophilic moiety D_5, was also synthesized in a similar way and exposed to thiol species to make a control for TPE-SS-D_5. The NMR and mass spectra analyses confirmed the right structures of TPE-NH_2, TPE-SS-D_5, and TPE-SS-COOH. (Figures S9–S13, Supporting Information)

To examine the potential of the TPE-SS-D_5 probe for thiol detection, GSH was selected as a representative thiol analyte due to its great importance and high concentration in biological systems.[52,53] First, 1.0 mM GSH was incubated with 10 μM TPE-SS-D_5 in DMSO/H_2O (v/v = 1/199) mixtures, and the fluorescence spectra were collected at different times. The fluorescence of the TPE-SS-D_5 probe is very weak in aqueous media. It increases significantly within the first 90 min, which is followed by saturation at 180 min (Figure 6A and Figure S14, Supporting Information). The effect of GSH concentration on the fluorescence of TPE-SS-D_5 was then examined by incubation of the probe with an increasing concentration of GSH from 5 to 1000 μM for 3 h; the corresponding spectra are shown in Figure 6B. Upon addition of GSH, the fluorescence gradually increases due to the cleavage of the disulfide bond and aggregate formation in aqueous solution. By plotting the PL intensities at 465 nm for TPE-SS-D_5 against the GSH concentration, a linear line is obtained (Figure 6C), suggesting the potential of using the probe for GSH quantification with a detection limit of 4.26 μM. The concentration-dependent experiments were also carried out using 90 min as the incubation time. There is a good linear relationship between the fluorescence intensity and the concentration of GSH (Figure S15A,B, Supporting Information). To further confirm the detection mechanism, reverse-phase HPLC and MS analyses were employed to monitor the fluorescence activation of the detection after incubation of TPE-SS-D_5 with GSH for 3 h. TPE-SS-D_5 itself has a retention time of 10.7 min, while the cleaved products have retention times of 14.6 and 15.6 min, as shown in Figure S16A,B (Supporting Information). The molecular weight of the cleaved species TPE-GSS and TPE-SH (structures shown in Figures S17 and S18, Supporting Information) were confirmed by ESI-MS,[54] indicating that the

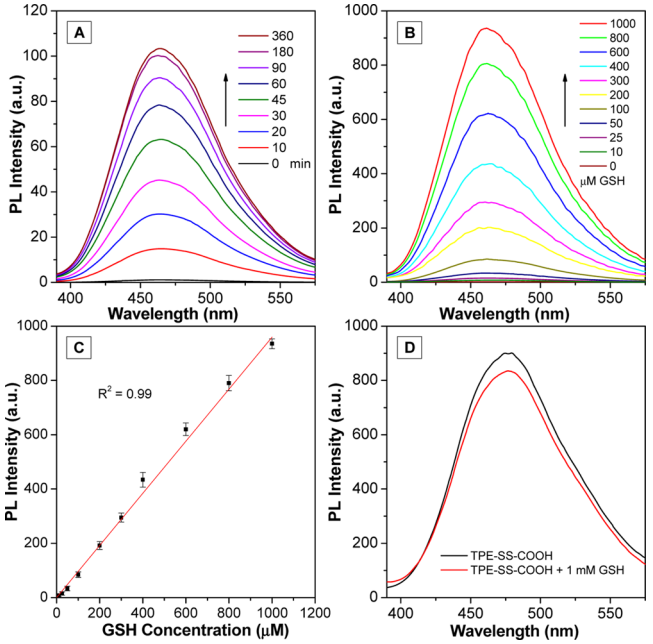

Figure 6. (A) Time-dependent PL spectra of 10 μM TPE-SS-D_5 treated with GSH (1.0 mM). (B) PL spectra of 1.0 mM TPE-SS-D_5 upon addition of increasing amounts of GSH from 0 to 1000 μM; incubation time, 180 min. (C) Plot of PL intensities of 1.0 mM TPE-SS-D_5 in DMSO/H_2O (v/v = 1/199) at 465 nm versus increasing amount of GSH (mean ± SD, n = 3). (D) PL spectra of 1.0 mM TPE-SS-COOH upon addition of 0 μM and 1 mM GSH DMSO/H_2O (v/v = 1/199). λ_{ex} = 304 nm for both TPE-SS-D_5 and TPE-SS-COOH.

fluorescence turn-on is due to the specific cleavage of the disulfide bond and the aggregation of hydrophobic TPE-SH. On the other hand, although TPE-SS-COOH could also be cleaved in the presence of GSH (Figure S16C,D, Supporting Information), its fluorescence intensity only shows very minor change due to the subtle variation in hydrophobicity before and after probe cleavage (Figure 6D). These results highlight the importance of the hydrophilic moiety D_5 in the design of light-

up probes and also validate the potential of the TPE-SS-D_5 probe for thiol detection.

CONCLUSION

In summary, we report a general strategy to fine tune the aggregation-induced emission characteristics of TPE−peptide conjugates for the development of fluorescence "turn-on" probes. With the number of carboxyl groups increasing from one to six, the fluorescence of TPE-D_n (n = 1−5) in aqueous media gradually decreased. Five carboxyl groups were found to be optimal to "turn off" the fluorescence of TPE. A proof-of-concept bioprobe TPE-SS-D_5 was used to validate our design by incorporating a cleavable disulfide linker between the hydrophilic moiety D_5 and TPE. The hydrophilic peptide moiety renders the AIE probe water-soluble, which allows it to be used in aqueous media with low background signal and a high fluorescence turn-on response to analyte. In addition, this strategy offers an effective solution to overcome the existing limitation of ligand selection for AIE probe design, enabling the development of more versatile bioprobes with hydrophobic recognition elements. The single labeling of the AIE probe also offers simplicity and reduced cost as compared to fluorophore and quencher dual labeled probes for realizing light-up sensing.

ASSOCIATED CONTENT

Supporting Information

Synthesis and characterization of intermediates and probe; PL spectra of TPE-NCS and TPE-D_n (n = 1−5) in DMSO/H_2O mixtures with different water fractions; HPLC spectra of TPE-SS-D_5, TPE-SS-COOH, and their product after incubation with GSH, and PL spectra of TPE-SS-D_5 upon addition of increasing concentrations of GSH with incubation time of 90 min. This material is available free of charge via the Internet at http://pubs.acs.org.

AUTHOR INFORMATION

Corresponding Author

*E-mail: cheliub@nus.edu.sg.

Notes

The authors declare no competing financial interest.

ACKNOWLEDGMENTS

We thank the Singapore National Research Foundation (R-279-000-390-281), the SMART program (R279-000-378-592), the Research Grants Council of Hong Kong (HKUST2/CRF/10 and N_HKUST620/11), and the Guangdong Innovative Research Team Program (201101C0105067115).

REFERENCES

(1) Lavis, L. D.; Raines, R. T. Bright Ideas for Chemical Biology. *ACS Chem. Biol.* **2008**, *3*, 142−155.
(2) Stich, M. I.; Fischer, L. H.; Wolfbeis, O. S. Multiple Fluorescent Chemical Sensing and Imaging. *Chem. Soc. Rev.* **2010**, *39*, 3102−3114.
(3) Schäferling, M. The Art of Fluorescence Imaging with Chemical Sensors. *Angew. Chem., Int. Ed.* **2012**, *51*, 3532−3554.
(4) Ueno, T.; Nagano, T. Fluorescent Probes for Sensing and Imaging. *Nat. Methods* **2011**, *8*, 642−645.
(5) Callan, J. F.; de Silva, A. P.; Magri, D. C. Luminescent Sensors and Switches in the Early 21st Century. *Tetrahedron* **2005**, *61*, 8551−8588.
(6) Kaur, K.; Saini, R.; Kumar, A.; Luxami, V.; Kaur, N.; Singh, P.; Kumar, S. Chemodosimeters: An Approach for Detection and Estimation of Biologically and Medically Relevant Metal Ions, Anions, and Thiols. *Coord. Chem. Rev.* **2012**, *256*, 1992−2028.
(7) Guo, H.; Jing, Y.; Yuan, X.; Ji, S.; Zhao, J.; Li, X.; Kan, Y. Highly Selective Fluorescent OFF−ON Thiol Probes Based on Dyads of BODIPY and Potent Intramolecular Electron Sink 2,4-Dinitrobenzenesulfonyl Subunits. *Org. Biomol. Chem.* **2011**, *9*, 3844−3853.
(8) Goswami, S.; Sen, D.; Das, N. K. A New, Highly Selective, Ratiometric and Colorimetric Fluorescence Sensor for Cu^{2+} with a Remarkable Red Shift in Absorption and Emission Spectra Based on Internal Charge Transfer. *Org. Lett.* **2010**, *12*, 856−859.
(9) Qian, X.; Xiao, Y.; Xu, Y.; Guo, X.; Qian, J.; Zhu, W. "Alive" Dyes as Fluorescent Sensors: Fluorophore, Mechanism, Receptor, and Images in Living Cells. *Chem. Commun.* **2010**, *46*, 6418−6436.
(10) Sapsford, K. E.; Berti, L.; Medintz, I. L. Materials for Fluorescence Resonance Energy Transfer Analysis: Beyond Traditional Donor−Acceptor Combinations. *Angew. Chem., Int. Ed.* **2006**, *45*, 4562−4589.
(11) Carlson, H. J.; Campbell, R. E. Genetically Encoded FRET-Based Biosensors for Multiparameter Fluorescence Imaging. *Curr. Opin. Biotechnol.* **2009**, *20*, 19−27.
(12) Liu, B.; Bazan, G. C. Homogeneous Fluorescence-Based DNA Detection with Water-Soluble Conjugated Polymers. *Chem. Mater.* **2004**, *16*, 4467−4476.
(13) Shao, J.; Sun, H.; Guo, H.; Ji, S.; Zhao, J.; Wu, W.; Yuan, X.; Zhang, C.; James, T. D. A Highly Selective Red-Emitting FRET Fluorescent Molecular Probe Derived from BODIPY for the Detection of Cysteine and Homocysteine: An Experimental and Theoretical Study. *Chem. Sci.* **2012**, *3*, 1049−1061.
(14) Sabelle, S.; Renard, P.-Y.; Pecorella, K.; de Suzzoni-Dézard, S.; Créminon, C.; Grassi, J.; Mioskowski, C. Design and Synthesis of Chemiluminescent Probes for the Detection of Cholinesterase Activity. *J. Am. Chem. Soc.* **2002**, *124*, 4874−4880.
(15) Thomas, S. W.; Joly, G. D.; Swager, T. M. Chemical Sensors Based on Amplifying Fluorescent Conjugated Polymers. *Chem. Rev.* **2007**, *107*, 1339−1386.
(16) Jun, M. E.; Roy, B.; Ahn, K. H. "Turn-On" Fluorescent Sensing with "Reactive" Probes. *Chem. Commun.* **2011**, *47*, 7583−7601.
(17) Luo, J. D.; Xie, Z. L.; Lam, J. W.; Cheng, L.; Chen, H. Y.; Qiu, C. F.; Zhu, D. B.; Tang, B. Z. Aggregation-Induced Emission of 1-Methyl-1,2,3,4,5-pentaphenylsilole. *Chem. Commun.* **2001**, *18*, 1740−1741.
(18) Tang, B. Z.; Zhan, X. W.; Yu, G.; Lee, P. S.; Liu, Y. Q.; Zhu, D. B. Efficient Blue Emission from Siloles. *J. Mater. Chem.* **2001**, *11*, 2974−2978.
(19) Chi, Z.; Zhang, X.; Xu, B.; Zhou, X.; Ma, C.; Zhang, Y.; Liu, S.; Xu, J. Recent Advances in Organic Mechanofluorochromic Materials. *Chem. Soc. Rev.* **2012**, *41*, 3878−3896.
(20) Zhang, X.; Zhang, X.; Tao, L.; Chi, Z.; Xu, J.; Wei, Y. Aggregation Induced Emission-Based Fluorescent Nanoparticles: Fabrication Methodologies and Biomedical Applications. *J. Mater. Chem. B* **2014**, *2*, 4398−4414.
(21) Hong, Y.; Lam, J. W. Y.; Tang, B. Z. Aggregation-Induced Emission: Phenomenon, Mechanism, and Applications. *Chem. Commun.* **2009**, *29*, 4332−4353.
(22) Hong, Y.; Lam, J. W.; Tang, B. Z. Aggregation-Induced Emission. *Chem. Soc. Rev.* **2011**, *40*, 5361−88.
(23) Parrott, E. P. J.; Tan, N. Y.; Hu, R.; Zeitler, J. A.; Tang, B. Z.; Pickwell-MacPherson, E. Direct Evidence to Support the Restriction of Intramolecular Rotation Hypothesis for the Mechanism of Aggregation-Induced Emission: Temperature Resolved Terahertz Spectra of Tetraphenylethene. *Mater. Horiz.* **2014**, *1*, 251−258.
(24) Ding, D.; Li, K.; Liu, B.; Tang, B. Z. Bioprobes Based on AIE Fluorogens. *Acc. Chem. Res.* **2013**, *46*, 2441−2453.
(25) Wang, M.; Zhang, G.; Zhang, D.; Zhu, D.; Tang, B. Z. Fluorescent Bio/Chemosensors Based on Silole and Tetraphenylethene Luminogens with Aggregation-Induced Emission Feature. *J. Mater. Chem.* **2010**, *20*, 1858−1867.
(26) Tong, H.; Hong, Y.; Dong, Y.; Häussler, M.; Li, Z.; Lam, J. W.; Dong, Y.; Sung, H. H. Y.; Williams, I. D.; Tang, B. Z. Protein

Detection and Quantitation by Tetraphenylethene-Based Fluorescent Probes with Aggregation-Induced Emission Characteristics. *J. Phys. Chem. B* **2007**, *111*, 11817−11823.
(27) Tong, H.; Hong, Y.; Dong, Y.; Häußler, M.; Lam, J. W.; Li, Z.; Guo, Z.; Guo, Z.; Tang, B. Z. Fluorescent "Light-Up" Bioprobes Based on Tetraphenylethylene Derivatives with Aggregation-Induced Emission Characteristics. *Chem. Commun.* **2006**, *35*, 3705−3707.
(28) Chen, X. T.; Xiang, Y.; Li, N.; Song, P. S.; Tong, A. J. Fluorescence Turn-On Detection of Protamine Based on Aggregation-Induced Emission Enhancement Characteristics of 4-(6′-Carboxyl)-hexyloxysalicylaldehyde Azine. *Analyst* **2010**, *135*, 1098−1105.
(29) Peng, L.; Zhang, G.; Zhang, D.; Xiang, J.; Zhao, R.; Wang, Y.; Zhu, D. A Fluorescence "Turn-On" Ensemble for Acetylcholinesterase Activity Assay and Inhibitor Screening. *Org. Lett.* **2009**, *11*, 4014−4017.
(30) Chen, J.; Jiao, H.; Li, W.; Liao, D.; Zhou, H.; Yu, C. Real-Time Fluorescence Turn-On Detection of Alkaline Phosphatase Activity with a Novel Perylene Probe. *Chem.—Asian J.* **2013**, *8*, 276−281.
(31) Wang, Y. Y.; Zhang, Y.; Liu, B. Conjugated Polyelectrolyte Based Fluorescence Turn-On Assay for Real-Time Monitoring of Protease Activity. *Anal. Chem.* **2010**, *82*, 8604−8610.
(32) Wang, M.; Gu, X.; Zhang, G.; Zhang, D.; Zhu, D. Convenient and Continuous Fluorometric Assay Method for Acetylcholinesterase and Inhibitor Screening Based on the Aggregation-Induced Emission. *Anal. Chem.* **2009**, *81*, 4444−4449.
(33) Xue, W.; Zhang, G.; Zhang, D.; Zhu, D. A New Label-Free Continuous Fluorometric Assay for Trypsin and Inhibitor Screening with Tetraphenylethene Compounds. *Org. Lett.* **2010**, *12*, 2274−2277.
(34) Wang, M.; Zhang, D.; Zhang, G.; Tang, Y.; Wang, S.; Zhu, D. Fluorescence Turn-On Detection of DNA and Label-Free Fluorescence Nuclease Assay Based on the Aggregation-Induced Emission of Silole. *Anal. Chem.* **2008**, *80*, 6443−6448.
(35) Wang, M.; Zhang, D.; Zhang, G.; Zhu, D. The Convenient Fluorescence Turn-On Detection of Heparin with a Silole Derivative Featuring an Ammonium Group. *Chem. Commun.* **2008**, *37*, 4469−4471.
(36) Kwok, R. T.; Geng, J.; Lam, J. W.; Zhao, E.; Wang, G.; Zhan, R.; Liu, B.; Tang, B. Z. Water-Soluble Bioprobes With Aggregation-Induced Emission Characteristics For Light-Up Sensing of Heparin. *J. Mater. Chem. B* **2014**, *2*, 4134−4141.
(37) Li, X.; Zhang, X.; Chi, Z.; Chao, X.; Zhou, X.; Zhang, Y.; Liu, S.; Xu, J. Simple Fluorescent Probe Derived from Tetraphenylethylene and Benzoquinone for Instantaneous Biothiol Detection. *Anal. Methods* **2012**, *4*, 3338−3343.
(38) Mei, J.; Tong, J. Q.; Wang, J.; Qin, A. J.; Sun, J. Z.; Tang, B. Z. Discriminative Fluorescence Detection of Cysteine, Homocysteine, and Glutathione via Reaction-Dependent Aggregation of Fluorophore-Analyte Adducts. *J. Mater. Chem.* **2012**, *22*, 17063−17070.
(39) Mei, J.; Wang, Y.; Tong, J.; Wang, J.; Qin, A.; Sun, J. Z.; Tang, B. Z. Discriminatory Detection of Cysteine and Homocysteine Based on Dialdehyde-Functionalized Aggregation-Induced Emission Fluorophores. *Chem.—Eur. J.* **2013**, *19*, 613−620.
(40) Lou, X.; Hong, Y.; Chen, S.; Leung, C. W. T.; Zhao, N.; Situ, B.; Lam, J. W. Y.; Tang, B. Z. A Selective Glutathione Probe Based on AIE Fluorogen and Its Application in Enzymatic Activity Assay. *Sci. Rep.* **2014**, *4*, 4272.
(41) Shi, H.; Liu, J.; Geng, J.; Tang, B. Z.; Liu, B. Specific Detection of Integrin $\alpha_v\beta_3$ by Light-Up Bioprobe with Aggregation-Induced Emission Characteristics. *J. Am. Chem. Soc.* **2012**, *134*, 9569−9572.
(42) Shi, H.; Kwok, R. T.; Liu, J.; Xing, B.; Tang, B. Z.; Liu, B. Real-Time Monitoring of Cell Apoptosis and Drug Screening Using Fluorescent Light-Up Probe with Aggregation-Induced Emission Characteristics. *J. Am. Chem. Soc.* **2012**, *134*, 17972−17981.
(43) Shi, H.; Zhao, N.; Ding, D.; Liang, J.; Tang, B. Z.; Liu, B. Fluorescent Light-Up Probe with Aggregation-Induced Emission Characteristics for in Vivo Imaging of Cell Apoptosis. *Org. Biomol. Chem.* **2013**, *11*, 7289−7296.
(44) Ding, D.; Liang, J.; Shi, H.; Kwok, R. T.; Gao, M.; Feng, G.; Yuan, Y.; Tang, B. Z.; Liu, B. Light-Up Bioprobe with Aggregation-Induced Emission Characteristics for Real-Time Apoptosis Imaging in Target Cancer Cells. *J. Mater. Chem. B* **2014**, *2*, 231−238.
(45) Yuan, Y.; Kwok, R. T.; Tang, B. Z.; Liu, B. Targeted Theranostic Platinum (IV) Prodrug with a Built-In Aggregation-Induced Emission Light-Up Apoptosis Sensor for Noninvasive Early Evaluation of Its Therapeutic Responses in Situ. *J. Am. Chem. Soc.* **2014**, *136*, 2546−2554.
(46) Huang, Y.; Hu, F.; Zhao, R.; Zhang, G.; Yang, H.; Zhang, D. Tetraphenylethylene Conjugated with a Specific Peptide as a Fluorescence Turn-On Bioprobe for the Highly Specific Detection and Tracing of Tumor Markers in Live Cancer Cells. *Chem.—Eur. J.* **2014**, *20*, 158−164.
(47) Wang, Z.; Chen, S.; Lam, J. W.; Qin, W.; Kwok, R. T.; Xie, N.; Hu, Q.; Tang, B. Z. Long-Term Fluorescent Cellular Tracing by the Aggregates of AIE Bioconjugates. *J. Am. Chem. Soc.* **2013**, *135*, 8238−8245.
(48) Yuan, Y.; Kwok, R. T.; Feng, G.; Liang, J.; Geng, J.; Tang, B. Z.; Liu, B. Rational Design of Fluorescent Light-Up Probes Based on An AIE Luminogen for Targeted Intracellular Thiol Imaging. *Chem. Commun.* **2014**, *50*, 295−297.
(49) Shiu, W. Y.; Mackay, D. A Critical Review of Aqueous Solubilities, Vapor Pressures, Henry's Law Constants, and Octanol−Water Partition Coefficients of the Polychlorinated Biphenyls. *J. Phys. Chem. Ref. Data* **1986**, *15*, 911−929.
(50) Miller, M. M.; Wasik, S. P.; Huang, G. L.; Shiu, W. Y.; Mackay, D. Relationships Between Octanol−Water Partition Coefficient and Aqueous Solubility. *Environ. Sci. Technol.* **1985**, *19*, 522−529.
(51) Levin, V. A. Relationship of Octanol/Water Partition Coefficient and Molecular Weight to Rat Brain Capillary Permeability. *J. Med. Chem.* **1980**, *23*, 682−684.
(52) Wu, G.; Fang, Y. Z.; Yang, S.; Lupton, J. R.; Turner, N. D. Glutathione Metabolism and Its Implications for Health. *J. Nutr.* **2004**, *134*, 489−492.
(53) Sies, H. Glutathione and Its Role in Cellular Functions. *Free Radical Biol. Med.* **1999**, *27*, 916−921.
(54) Jocelyn, P. The Standard Redox Potential of Cysteine-Cystine from the Thiol-Disulphide Exchange Reaction with Glutathione and Lipoic Acid. *Eur. J. Biochem.* **1967**, *2*, 327−331.